

# Mean Field Studies of Exotic Nuclei

C. R. Chinn

*Department of Physics and Astronomy Vanderbilt University, Nashville, TN 37235*

A. S. Umar

*Department of Physics and Astronomy Vanderbilt University, Nashville, TN 37235  
and Center for Computationally Intensive Physics, Oak Ridge National  
Laboratory, Oak Ridge, TN 37831-6373*

M. Vallières,

*Department of Physics and Atmospheric Sciences, Drexel University, Philadelphia,  
PA 19104*

M. R. Strayer

*Physics Division, Oak Ridge National Laboratory Oak Ridge, Tennessee 37831 and  
Center for Computationally Intensive Physics, Oak Ridge National Laboratory,  
Oak Ridge, TN 37831-6373*

---

## Abstract

Full three dimensional static and dynamic mean field calculations using collocation basis splines with a Skyrme type Hamiltonian are described. This program is developed to address the difficult theoretical challenges offered by exotic nuclei. Ground state and deformation properties are calculated using static Hartree-Fock, Hartree-Fock+BCS and constrained Hartree-Fock models. Collective properties, such as reaction rates and resonances, are described using a new alternate method for evaluating linear response theory, which is constructed directly on top of the static calculation. This provides a consistent description of the ground state, deformation and collective nuclear properties. Sample results are presented for the giant multiple resonances of  $^{16}\text{O}$ .

---

## 1 Introduction

With the recent and future advent of new experimental facilities, such as the Radioactive Ion Beams facility at ORNL and GammaSphere, exploratory

detailed studies of many exotic nuclei will need correspondingly accurate theoretical investigations. Examples of some of the properties of nuclei which will be studied include effective interactions, masses and ground state properties, multi-dimensional energy surfaces and reaction rates. The results of these studies may also impact and address many astrophysical questions.

The calculations discussed in this paper can be separated into two basic categories. These are static mean field theories, such as Hartree-Fock, Hartree-Fock-Bogolyubov and constrained Hartree-Fock calculations; and using dynamic linear response theory to study large-scale collective motion and reaction rates.

Because of new capabilities in computer technology as well as innovations in numerical algorithms, a much greater level of sophistication can be incorporated into numerical studies than in the past. In the studies presented in this paper, we incorporate the following ingredients. Collocation lattice representations using basis splines are used instead of traditional grid representations or basis expansions. A full unrestricted three-dimensional calculation is performed, where no assumptions about spatial symmetries are needed. Spin degrees are included and one need not impose time reversal symmetry. As a result, to study nuclei with a large number of single particle states one requires grand challenge level computing resources.

Collocation basis splines provide a superior representation than traditional grid techniques. The reason for this is that with basis splines, the gradient operator is represented as an operation upon a set of basis functions, which is much more accurate than the finite difference methods used in traditional calculations. At the same time collocation basis splines allow for the advantageous use of lattice representations. Here a full three-dimensional collocation lattice is used.

It may be argued that there are existing accurate mean field calculations which use alternate basis expansions, such as sets of harmonic oscillator functions. One finds though that although these methods provide for accurate studies of more traditional nuclei, when one addresses exotic nuclei near the drip lines, such calculations begin to fail to accurately represent the physics. This can be traced to the fact that exotic nuclei, because of small binding energies, have very extended density distributions. One finds the harmonic oscillators bases typically used, due to their natural locality, are less able to represent accurately such extended objects than can a grid representation [1].

An alternate method has been developed to solve the linear response theory, which is a refinement of the technique used in ref. [2]. Instead of solving a specific set of equations, the response of the system is derived using time-dependent Hartree-Fock [TDHF] theory. In this case a specific time-dependent

perturbing piece is added to the static hamiltonian to give  $H_{tot}(t)$ . The static Hartree-Fock solution is then time-evolved using  $H_{tot}(t)$  in a TDHF calculation. The Fourier transform of the result gives the response of the system at all energies. In this scheme one recovers both the response spectrum as well as the total transition probability amplitude corresponding to a given specific collective mode.

The main advantage of this approach is that the dynamical linear response calculation is constructed directly on top of the static Hartree-Fock calculation and hence the static and dynamical calculations are calculated using the same hamiltonian description and the same degree of complexity. Therefore, there is a complete consistency between the static ground state of the system and the response calculations. One can then provide a coherent description of static properties of nuclei and of dynamical properties. This is important for example in  $\beta$ -decay calculations of exotic nuclei, where reliable predictions are very sensitive to the deformation properties of the nucleus. Hence in this formalism consistent predictions of both the deformation and reaction rate properties are possible.

Pairing correlations can be included in both the static and dynamic formalisms. Presently, the BCS and Lipkin-Nogami prescriptions for including pairing have been used. Eventually we would like to use a self-consistent description of pairing correlations, which would enable us to perform quasi-RPA studies of  $\beta$ -decay for nuclei near the drip lines. With the recent advent of radioactive beam facilities, one would like to provide accurate and physical predictions of properties of exotic nuclei.

Section 2 contains the theoretical discussion. Results are given in Section 3 followed by a summary and conclusion in Section 4.

## 2 Theoretical Discussion

### 2.1 Continuous Equations

The details of the derivation of the Hartree-Fock equations can be found in [3,4,5,6]. The result for a many-body Hamiltonian containing a one-body kinetic energy and two- and three-body momentum dependent potential terms is a coupled set of non-linear partial differential eigenvalue equations,

$$\mathbf{h}\chi_\alpha = \epsilon_\alpha \chi_\alpha , \quad \chi_\alpha = \begin{pmatrix} \chi_\alpha^+ \\ \chi_\alpha^- \end{pmatrix} , \quad (1)$$

where  $\chi_\alpha$  is a two-component vector (spinor). The effective nucleon-nucleon interaction is chosen to be of the zero-range Skyrme type, hence the Hamiltonian  $\mathbf{h}$  can be written in the following form (using natural units  $\hbar = 1$ ,  $c = 1$ ,  $m = 1$ )

$$\begin{aligned} \mathbf{h} &= -\frac{1}{2}\vec{\nabla}^2 + W(\rho, \tau, \vec{j}, \vec{J}), \\ W &= V_N(\vec{r}) + V_C(\vec{r}), \end{aligned} \quad (2)$$

where  $V_N$  is the nuclear potential depending on various currents and densities and  $V_C$  is the Coulomb interaction. The densities and currents depend on the states  $\chi_\alpha$  and are explicitly given by

$$\rho(\vec{r}) = \sum_\alpha w_\alpha \{ |\chi_\alpha^+(\vec{r})|^2 + |\chi_\alpha^-(\vec{r})|^2 \} \quad (3)$$

$$\tau(\vec{r}) = \sum_\alpha w_\alpha \{ |\nabla \chi_\alpha^+(\vec{r})|^2 + |\nabla \chi_\alpha^-(\vec{r})|^2 \} \quad (4)$$

$$\vec{j}(\vec{r}) = \sum_\alpha w_\alpha \{ Im[\chi_\alpha^{+*}(\vec{r}) \vec{\nabla} \chi_\alpha^+(\vec{r}) + \chi_\alpha^{-*}(\vec{r}) \vec{\nabla} \chi_\alpha^-(\vec{r})] \} \quad (5)$$

$$\vec{J}(\vec{r}) = -i \sum_{\substack{\alpha \\ \mu \mu' = \pm}} w_\alpha \chi_\alpha^{\mu*}(\vec{r}) (\vec{\nabla} \times \vec{\sigma}) \chi_\alpha^{\mu'}(\vec{r}) . \quad (6)$$

$V_C$  requires the solution of the Poisson equation in three-dimensional geometry,

$$\nabla^2 V_C(\vec{r}) = -4\pi e^2 \rho(\vec{r}) . \quad (7)$$

As can be seen from above, the solution of the system of equations (1) has to be obtained self-consistently and an accurate solution requires a good representation of various derivatives of the states  $\chi_\alpha$ . Currently, most HF and TDHF calculations are performed using finite difference lattice techniques. It is desirable to investigate higher-order interpolation methods which result in the improvement of the overall accuracy and reduction in the total number of lattice points. The lattice solution of differential equations on a discretized mesh of independent variables may be viewed to proceed in two steps: (1) Obtain a discrete representation of the functions and operators on the lattice. (2) Solve the resulting lattice equations using iterative techniques. Step (1) is an interpolation problem for which we could take advantage of the techniques developed using the spline functions [7,8,9]. The use of the spline collocation method leads to a matrix-vector representation on the collocation lattice with a metric describing the transformation properties of the collocation lattice.

## 2.2 Solution of the Discrete HF Equations

The solution of the HF equations (1) is found by using the damped relaxation method described in Refs. [10,11]

$$\chi_{\alpha}^{k+1} = \mathcal{O} \left[ \chi_{\alpha}^k - x_0 \mathbf{D}(E_0) \left( \mathbf{h}^k - \epsilon_{\alpha}^k \right) \chi_{\alpha}^k \right] , \quad (8)$$

where  $\mathcal{O}$  stands for Gram-Schmidt orthonormalization. The preconditioning operator  $\mathbf{D}$  is chosen to be [10,11]

$$\begin{aligned} \mathbf{D}(E_0) &= \left[ 1 + \frac{\mathbf{T}}{E_0} \right]^{-1} \\ &\approx \left[ 1 + \frac{\mathbf{T}_x}{E_0} \right]^{-1} \left[ 1 + \frac{\mathbf{T}_y}{E_0} \right]^{-1} \left[ 1 + \frac{\mathbf{T}_z}{E_0} \right]^{-1} , \end{aligned}$$

where  $\mathbf{T}$  denotes the kinetic energy operator. The solution is obtained through an iterative scheme as outlined below:

- (i) Guess a set of orthogonal single-particle states
- (ii) Compute the densities (6)
- (iii) Compute the Hartree-Fock potential
- (iv) Solve the Poisson equation
- (v) Perform a damping step (8) without orthogonalization
- (vi) Do a Gram-Schmidt orthogonalization of all states
- (vii) Repeat beginning at step (ii) until convergence

In practical calculations we have used the damping scale value  $x_0 \approx 0.05$  and the energy cutoff  $E_0 \approx 20.0$ . As a convergence criteria we have required the fluctuations in energy

$$\Delta E^2 \equiv \sqrt{\langle H^2 \rangle - \langle H \rangle^2} \quad (9)$$

to be less than  $10^{-5}$ . This is a more stringent condition than the simple energy difference between two iterations, which is about  $10^{-10}$  when the fluctuation accuracy is satisfied. The calculation of the HF Hamiltonian also requires the evaluation of the Coulomb contribution given by Eq. (7). Details of solving the Poisson equations using the splines are given in Ref. [8,9].

## 2.3 Collocation Basis Splines

The static and time-dependent Hartree-Fock calculations are performed using a collocation spline basis in a three-dimensional lattice configuration. Basis

splines allow for the use of a lattice grid representation of the nucleus, which is much easier to use than alternate basis techniques, such as multi-dimensional harmonic oscillators. Also, for studies of exotic nuclei, because of weak binding, the density distributions tend to extend to large distances and hence one finds a large sensitivity to a harmonic oscillator basis, while for a lattice grid representation one needs to simply increase the size of the box. Traditional grid representations typically use finite difference techniques to represent the gradient operator. Collocation basis splines allow for the gradient operator to be represented by its action upon a basis function in a matrix form. This collocation method gives a much more accurate representation of the gradient, while maintaining the convenience of a lattice grid and hence provides a much more accurate calculation in the end.

An  $M$ th order spline function denoted by  $B_i^M$  is constructed from piecewise continuous polynomials up to order  $M - 1$ . The set of points or *knots*  $\{x_i\}$  consists of the points where the spline functions are joined continuously up to the  $(M - 2)$  derivative. The basis spline functions have minimal support in that the  $i$ th spline functions is nonzero only in the interval  $(x_i, x_{i+M})$ , where the spline function,  $B_i^M$ , is labelled by the first knot. For the case of using static boundary conditions for the space containing the  $N + 1$  knots in one dimension, there must be  $M$  nonzero spline functions in each interval, hence  $N + 2M - 1$  total spline functions make up the full basis, where  $M - 1$  spline functions extend beyond each boundary. One can also impose periodic boundary conditions, where there will then be  $N$  total spline functions.

A function,  $f(x)$  continuous in the interval  $(x_{min}, x_{max})$  is expanded in terms of the spline basis functions:

$$f(x) = \sum_i^{N+2M-1} B_i^M(x) c^i. \quad (10)$$

The expansion coefficients,  $c^i$  are derived from  $f(x)$  by evaluating  $f(x)$  at a specific set of points called *collocation points*,  $\{x'_\alpha\}$ . There are various ways of choosing the  $\{x'_\alpha\}$ . For odd order splines we have chosen the collocation points to lie at the center of each knot interval within the range  $(x_{min}, x_{max})$ .

$$x_{min} = x_M, \\ x'_\alpha = \frac{x_{i+M-1} + x_{i+M}}{2}, \quad i = \alpha, \quad \forall \alpha = 1, \dots, N$$

By evaluating eq. (10) at  $\{x'_\alpha\}$ , a set of linear equations are constructed which constrain the coefficients,  $c^i$ :

$$f(x'_\alpha) = \sum_i^{N+2M-1} B_i^M(x'_\alpha) c^i. \quad (11)$$

Since there are  $N+2M-1$  unknown coefficients in the case of static boundary conditions and  $N$  points  $x'_\alpha$ , it is necessary to introduce  $2M-1$  additional constraining equations as boundary conditions. Combining the functions  $B_i^M(x'_\alpha)$  and the boundary conditions into a square invertible matrix,  $\mathbf{B}$ , the coefficients,  $c^i$  can be expressed as:

$$c^i = \sum_{\alpha} \left[ \mathbf{B}^{-1} \right]^{i\alpha} f_{\alpha}, \quad (12)$$

where  $f_{\alpha} \equiv f(x'_\alpha)$  is the collocation representation of the function,  $f(x)$ .

Consider the action of an operator upon a function:

$$\hat{O}f(x) = \sum_i^{N+2M-1} \left[ \hat{O}B_i^M(x) \right] c^i. \quad (13)$$

If we evaluate the above expression at the collocation points and substitute in eq. (12) for the  $c^i$  the following is obtained.

$$\hat{O}f(x'_\alpha) = \hat{O}f_{\alpha} = \sum_i^{N+2M-1} \left[ \hat{O}B_i^M(x'_\alpha) \right] \sum_{\beta} \left[ \mathbf{B}^{-1} \right]^{i\beta} = \sum_{\beta} \hat{O}_{\alpha}^{\beta} f_{\beta}, \quad (14)$$

where now the quantity,  $\hat{O}_{\alpha}^{\beta}$  is the collocation representation of the operator,  $\hat{O}$  on the lattice.

$$\hat{O}_{\alpha}^{\beta} \equiv \sum_i^{N+2M-1} \left[ \hat{O}B_i^M(x'_\alpha) \right] \left[ \mathbf{B}^{-1} \right]^{i\beta} \quad (15)$$

Note that the representation,  $\hat{O}_{\alpha}^{\beta}$ , is not a sparse matrix.

The function,  $f(x)$ , and the operator,  $\hat{O}$ , can both be represented on a lattice, *i.e.* the collocation points, through the use of the collocation basis spline method. This holds true for gradient operators, where the gradient of the basis spline functions is required. The basis spline functions,  $B_i^M(x)$  and their derivatives,  $\frac{\partial^n B_i^M(x)}{\partial x^n}$  can be evaluated at the collocation points using iterative techniques. Through similar methods one can obtain the appropriate integration weights:

$$I = \int_a^b f(x) dx = \sum_{\alpha} w_{\alpha} f(x_{\alpha}), \quad (16)$$

where the weights are given as :

$$w^\alpha \equiv \sum_i^{N+2M-1} \int_a^b B_i^M(x) dx \left[ \mathbf{B}^{-1} \right]^{i\alpha}. \quad (17)$$

For more details on the collocation basis spline method please see Ref. [9].

#### 2.4 Linear Response Theory

The linear response equations can be derived from a specific functional time-dependent perturbation of the TDHF equations [12]. To begin the proof a solution to the static Schrödinger equation is written as follows:

$$\widehat{H}|\psi_s(0)\rangle = E|\psi_s(0)\rangle. \quad (18)$$

A time-dependent perturbing function is added to the static hamiltonian:

$$\widehat{H}_{tot} = \widehat{H} + \widehat{H}_{ex}(t). \quad (19)$$

The external piece is defined as:

$$\begin{aligned} \widehat{H}_{ex}(t) &= \widehat{F}f(t) \\ &= \left[ \int d^3x \widehat{n}(x, t) F(x) \right] f(t), \end{aligned} \quad (20)$$

where  $\widehat{n}(x, t)$  is the number density operator.  $F(x)$  corresponds to some particular collective mode. The functions,  $F(x)$  and  $f(t)$  will be chosen later.

At some time  $t = t_0$  the external piece of the Hamiltonian is turned on where  $|\bar{\psi}_s(t)\rangle$  is the solution to the time-dependent Schrödinger equation:

$$i\hbar \frac{\partial}{\partial t} |\bar{\psi}_s(t)\rangle = \left[ \widehat{H} + \widehat{H}_{ex}(t) \right] |\bar{\psi}_s(t)\rangle. \quad (21)$$

Here the subscript ‘ $s$ ’ refers to the Schrödinger picture. The solution for the state vector can be written in the following iterative fashion.

$$|\bar{\psi}_s(t)\rangle = e^{-i\widehat{H}t/\hbar} |\psi_s(0)\rangle - \frac{i}{\hbar} e^{-i\widehat{H}t/\hbar} \int_{t_0}^t dt' \widehat{H}_{ex}^I(t') |\psi_s(0)\rangle + \dots, \quad (22)$$

where the superscript ‘ $I$ ’ refers to the interaction picture. The expectation value of any operator,  $\hat{O}(t)$ , is equal to

$$\begin{aligned} \langle \bar{\psi}_s(t) | \hat{O}_S(t) | \bar{\psi}_s(t) \rangle &= \langle \bar{\psi}_s(0) | \hat{O}_S(0) | \bar{\psi}_s(0) \rangle + \\ &+ \langle \bar{\psi}_s(0) | \frac{i}{\hbar} \int_{t_0}^t dt' \left[ \hat{H}_{ex}^I(t'), \hat{O}_I(t) \right] | \bar{\psi}_s(0) \rangle + \dots . \end{aligned} \quad (23)$$

The linear approximation is made such that terms beyond first order in  $\hat{H}_{ex}^I$  are neglected.

If we define the operator  $\hat{O}(t)$  to be the number density operator, then using eq. (20) the fluctuation in the density becomes:

$$\begin{aligned} \delta \langle \hat{n}(x, t) \rangle &= \langle \bar{\psi}_s(t) | \hat{O}_S(t) | \bar{\psi}_s(t) \rangle - \langle \bar{\psi}_s(0) | \hat{O}_S(0) | \bar{\psi}_s(0) \rangle \\ &= \langle \bar{\psi}_s(0) | \frac{i}{\hbar} \int_{t_0}^t dt' \int d^3x' F(x') f(t') [\hat{n}_I(x', t'), \hat{n}_I(x, t)] | \bar{\psi}_s(0) \rangle \end{aligned} \quad (24)$$

The retarded density correlation function is defined as:

$$iD^R(x, t; x', t') = \theta(t - t') \frac{\langle \psi_0 | [\tilde{n}_H(k), \tilde{n}_H(k')] | \psi_0 \rangle}{\langle \psi_0 | \psi_0 \rangle}, \quad (25)$$

where  $\tilde{n}_H = \hat{n}_H - \langle \hat{n}_H \rangle$  is the deviation of the number operator in the Heisenberg picture. The density fluctuation can be written as:

$$\delta \langle \hat{n}(x, t) \rangle = \frac{1}{\hbar} \int_{-\infty}^{\infty} dt' \int d^3x' D^R(x, t; x', t') F(x') f(t'). \quad (26)$$

Using the Fourier representation of  $\theta(t - t')$ , the Fourier transform of the density correlation function is:

$$\begin{aligned} iD^R(x, x'; \omega) &= \int_{-\infty}^{\infty} d(t - t') e^{i\omega(t - t')} iD^R(x, t; x', t') \\ &= \sum_n \left\{ \frac{\langle \psi_0 | \tilde{n}_S(\vec{x}) | \psi_n \rangle \langle \psi_n | \tilde{n}_S(\vec{x}') | \psi_0 \rangle}{\omega - \frac{E_n - E_0}{\hbar} + i\eta} - \frac{\langle \psi_0 | \tilde{n}_S(\vec{x}') | \psi_n \rangle \langle \psi_n | \tilde{n}_S(\vec{x}) | \psi_0 \rangle}{\omega + \frac{E_n - E_0}{\hbar} + i\eta} \right\}, \end{aligned}$$

where  $|\psi_n\rangle$  represents the full spectrum of excited many-body states of  $\hat{H}$ .

The Fourier transform of the density fluctuation then becomes:

$$\begin{aligned}
\delta\langle\hat{n}(x, \omega)\rangle &= \int_{-\infty}^{\infty} dt e^{i\omega t} \delta\langle n(x, t)\rangle \\
&= \frac{1}{\hbar} \int d^3 x' D^R(\vec{x}, \vec{x}'; \omega) F(x') f(\omega), \\
\text{where } f(\omega) &= \int_{-\infty}^{\infty} dt' e^{i\omega t'} f(t')
\end{aligned} \tag{28}$$

The linear response structure function,  $S(\omega)$  is derived to be:

$$\begin{aligned}
f(\omega) S(\omega) &= \int d^3 x \delta\langle F^\dagger(x) n(x, \omega)\rangle \\
&= \frac{1}{\hbar} \int d^3 x \int d^3 x' F^\dagger(\vec{x}) D^R(\vec{x}, \vec{x}'; \omega) F(\vec{x}') f(\omega).
\end{aligned} \tag{29}$$

Combining eqs. (27) and (29) the imaginary part of the structure function then gives the total transition probability associated with  $F(\vec{x})$ .

$$IM [S(\omega)] = -\frac{\pi}{\hbar} \sum_n \left| \int d^3 x' \langle \psi_n | \tilde{n}_x(\vec{x}') | \psi_0 \rangle F(\vec{x}') \right|^2 \delta\left(\omega - \frac{E_n - E_0}{\hbar}\right), \quad E_n \geq E_0. \tag{30}$$

Note that this quantity is purely negative, where this feature can be used as a measure of the convergence of the solution.

At this point instead of using the standard route of letting  $f(t) \rightarrow 0$  to recover the linear response equations, we choose an alternate technique to calculate the response. In this case we evolve the system in time and then fourier transform the result, where  $H_{ex}(t)$  is a perturbing function. In this case  $f(t)$  is chosen to be a Gaussian of the following form.

$$\begin{aligned}
f(t) &= \varepsilon e^{-\frac{\alpha}{2}(t-t_\alpha)^2}, \quad t \geq t_0 \\
f(\omega) &= \varepsilon \sqrt{\frac{2\pi}{\alpha}} e^{-\frac{\omega^2}{2\alpha} + i\omega t_\alpha},
\end{aligned} \tag{31}$$

where  $\varepsilon$  is some small number ( $\sim 10^{-5}$ ), chosen such that we are in the linear regime. The parameter,  $\alpha$ , is set to be  $\sim 1.0$  c/fm, which allows for a reasonable perturbation of collective energies up to  $\approx 150$  MeV. The offset in time,  $t_\alpha$  is chosen such that the full gaussian is approximately within the time regime,  $t \geq t_0$ .

In practice to evaluate the TDHF equations the time-evolution operator is used to evolve the system.

$$U(t, t_0) = T \left[ e^{-\frac{i}{\hbar} \int_{t_0}^t dt' \hat{H}_{tot}(t')} \right], \quad (32)$$

where  $T [ \dots ]$  denotes time-ordering. Using infinitesimal time increments, the time-evolution operator is approximated by

$$\begin{aligned} U(t_{n+1}, t_n) &= e^{-\frac{i}{\hbar} \int_{t_n}^{t_{n+1}} dt' \hat{H}_{tot}(t')} \\ &\approx e^{-\frac{i}{\hbar} \Delta t \hat{H}_{tot}(t_n + \frac{\Delta t}{2})} \\ &\approx 1 + \sum_{k=1}^N \left[ \frac{(-\frac{i}{\hbar} \Delta t \hat{H}_{tot})^k}{k!} \right], \end{aligned} \quad (33)$$

where the quantity  $\hat{H}_{tot}^k$  is evaluated by repeated operations of  $\hat{H}_{tot}$  upon the wave functions.

The procedure is to then choose a particular form for  $F(\vec{x})$ , using eq. (31) for  $f(t)$ , and time evolve the system using eq. (33). The Fourier transform in time of the result then gives us  $f(\omega)S(\omega)$ , from which the linear response structure function of the system is extracted. For a more detailed discussion please see Ref. [13].

### 3 Results

The static mean field calculation is analyzed in detail in Ref. [14]. For an example of some results using the static model in a HF+BCS calculation, please see Ref. [15], where the results for various sulphur isotopes are presented. The pairing correlations are described by using a constant gap approximation of 0.2 MeV.

The static and dynamic Hartree-Fock calculations are performed using a 3-dimensional collocation lattice constructed with B-splines. Typically a 7th order B-spline is used in a  $(-10, +10 \text{ fm})^3$  box with  $20^3 - 24^3$  grid points. The calculation can be performed with or without assuming time-reversal symmetry. The collective linear response may involve particle-hole interactions which are spin-dependent and not time-reversal symmetric. Therefore, for the correct collective content to be included one should not impose time-reversal symmetry in the linear response calculations [16]. In the results presented in this paper time-reversal symmetry is not imposed. In a comparison it is found

that imposing time-reversal symmetry causes small shifts in the position of the collective modes on the order of  $\approx 0.3$  MeV.

Calculations of isoscalar octupole; and isoscalar quadrupole collective modes are presented for  $^{16}\text{O}$  using several parametrizations of the Skyrme interaction. Here the parametrizations known as skm\* [17] and sgII [18] are used for comparisons. A time step of  $\Delta t = 0.4$  fm/c is used for the calculations. It is found that one can perform the time evolution for over 40000 time steps. The results shown here typically use 16384 time steps for a maximum time of  $\approx 6550$  fm/c.

Reasonable results are obtained if the parameter  $\varepsilon$  in eq. (31) is chosen to fall in the range  $2.0 \times 10^{-4} \leq \varepsilon \leq 2 \times 10^{-7}$ . By varying the value of  $\varepsilon$ , the amplitude of the time-dependent density fluctuation then scales proportionally to  $\varepsilon$ , thus indicating that we are well within the linear regime of the theory.

The linear response calculations require well converged initial static HF solutions. To test for the convergence of the static HF calculation the energy fluctuation, which is the variance of  $\widehat{H}$  as given in eq. (9), is minimized. This measure of convergence tests directly how close the wave functions are to being eigenstates of  $\widehat{H}$  and is independent of the iteration step size. For  $^{16}\text{O}$  it was found that static HF solutions with energy fluctuation less than about  $1.0 \times 10^{-5}$  provided adequate starting points for the dynamic calculation, although the smaller the energy fluctuation the better.

The dynamic calculations involve using eq. (33) to evolve the system. Since  $U(t, t')$  is an unitary operator, the orthonormality of the system is preserved, therefore it is not necessary to re-orthogonalize the solutions after every time-step. The stability of the calculation is checked by testing the preservation of the norm of each wave function. The number of terms in the expansion of the exponent in eq. (33) is determined by requiring the norm to be preserved to a certain accuracy (typically to  $\leq 5.0 \times 10^{-10} \rightarrow 1.0 \times 10^{-8}$ ).

The time-dependent perturbing part of the Hamiltonian is evaluated when the exponent in eq. (31) is greater than some small number,  $\varepsilon_{cut}$ . Since it is not difficult to evaluate the action of the external part of the Hamiltonian on the wave function,  $\varepsilon_{cut}$  is chosen to be very small, ( $1.0 \times 10^{-10}$ ). To allow the fourier transform of  $f(t)$  to be evaluated easily, it is necessary to integrate  $t$  from  $-\infty$  to  $\infty$  and hence we would like the entire Gaussian of the perturbing function,  $f(t)$ , to be included into the time evolution to the desired accuracy. The parameter  $t_\alpha$  is therefore chosen such that the complete nonzero contribution of the time-dependent perturbation is included.  $t_\alpha = \Delta t \left( 2 + \sqrt{\left| \frac{2 \log \varepsilon_{cut}}{\alpha \Delta t} \right|} \right)$ .

Pairing can be easily included using the BCS [19] or Lipkin-Nogami [20] constant pairing strength prescriptions. These two methods have been included

into the static Hartree-Fock calculations and can be easily incorporated into the dynamical calculation. For studies of  $\beta$ -decay it will be necessary to include pairing, thus producing calculations of responses to quasi-RPA excitation modes.

The computations were performed on massively parallel INTEL iPSC/860 and PARAGON supercomputers.

For the study of the isoscalar quadrupole moment, the perturbing function  $F(\vec{x})$ , introduced in eq. (20), is chosen to be the mass quadrupole moment,  $Q_{20} = 2z^2 - (x^2 + y^2)$ . It turns out that other even multipole modes are also excited at the same time (*i.e.*  $Q_{40}, Q_{60}, \dots$ ). One can therefore study the effect of the coupling between the different excitation modes. The same holds true for the odd multipoles.

In the top panel of Fig. 1 the time-dependent evaluation of the axial quadrupole moment,  $\langle \hat{Q}_{20}(t) \rangle$  is given for  $^{16}\text{O}$  using the skm\* parametrization.

$$\langle \hat{Q}_{20}(t) \rangle = \langle F(x) \rangle = \int d^3x \delta(\hat{n}(x, t)) F^\dagger(x), \quad (34)$$

In this case the box is set to be  $(-10, +10 \text{ fm})^3$  in size using  $20^3$  grid points. The periodic nature of the calculation is clear in this figure, where the smallest oscillation has a period of about  $65 \text{ fm}/c$ .

Both a discrete Fourier transform [FT] and a continuous FT via Filon's method are used to calculate the FT of  $\langle \hat{Q}_{20}(t) \rangle$  to give  $\langle \hat{Q}_{20}(\omega) \rangle = f(\omega) S_{20}(\omega)$ . The frequency grid,  $\Delta\omega$  is given by  $2\pi/T_{max}$ , so for a finer mesh one need only to time evolve to a larger maximum time,  $T_{max}$ . The continuous FT is also limited by this criteria. The discrete and continuous FT's give essentially identical spectrums, although the continuous FT recovers  $f(\omega)$  more precisely and appears to give a more reasonable energy-weighted sum rule [EWSR] result. One can use the analytic expression for  $f(\omega)$  given in eq. (31) or a numerical result, where the difference in the spectrum is negligible.

The lower panel shows the resulting response calculation. This quantity was derived in eq. (30) to be purely negative. The skm\* results reflect this property quite well, where one sharp peak is seen at about  $19.8 \text{ MeV}$ . The calculation recovers about 92% of the exact EWSR, indicating excellent convergence.

To test the sensitivity of the dynamic calculation to the box size, the calculation shown in Fig. 1 is repeated using two larger boxes. The result in Fig. 1 is compared in Fig. 2 to calculations using a box  $= (-11, +11 \text{ fm})^3$  with  $22^3$  grid points in the middle panel and one using a box  $= (-12, +12 \text{ fm})^3$  with  $24^3$  grid points in the lower panel. In all three cases the grid spacing is set to be  $1 \text{ fm}$ . One note is that since the continuum is represented by discrete

states in a box, the resonances are very sharply peaked. To best represent these peaks,  $T_{max}$  is adjusted and chosen to give frequency grid locations as close to the peaks as possible. In the top panel it ended up that  $N = 16384$ , where  $T_{max} = N \times \Delta t$ , is an ideal choice. For the other two panels we found that choosing larger  $T_{max}$ 's and hence larger  $N$ 's gave much better spectrums. One finds though that the spectrum changes as the box size is increased and in the middle panel there are 3 large peaks rather than just one. This disturbing result indicates that the spectrum as well as the peak positions appear to be significantly affected by the box size. We also find an effect when static boundary conditions are imposed instead of periodic ones.

In Fig. 3 a calculation similar to Fig. 2 is shown, where the sgII Skyrme force parametrization is used. In this case the box also has a large effect on the calculated spectrum. The peak positions shift as well as the number of peaks. Also shown in the middle panel is a calculation which uses  $22^3$  grid points but with a denser grid. In this case there is also a significant change in the spectrum.

The dependence observed in Figs. 2 and 3 can be traced to the representation of the continuum as given by the box. The lowest energy continuum states in the box correspond to the states with the fewest nodes. These states are of course dependent upon the size of the box. By increasing the size of the box, the lowest energy of these continuum states is reduced and the continuum is better represented in the calculation. Efforts are underway to increase the size of the box, by introducing unequal lattice spacing into the calculation.

In Fig.4 the isoscalar octupole response is shown for the skm\* and sgII effective interactions. There are 3 sharp resonance structures at about 6 – 7 MeV, 13 – 14 MeV and 18 MeV, where the sgII resonances are at the slightly higher energies. These three peaks are also found in a spherical RPA calculation using the same effective interactions [21]. The spherical calculation finds an additional broad peak for skm\* and sgII centered at an energy of about 27 – 28 MeV. This peak is weaker than the 3 peaks at lower energies and is not observed in the three-dimensional linear response calculation. In Fig. 4 one can see that the response is approximately purely negative, but that there are some violations of this feature.

#### 4 Summary and Conclusions

A method for evaluating the linear response theory using TDHF is formally developed and implemented. This method allows one to construct the dynamic calculation directly on top of the static Hartree-Fock calculation. Therefore, by performing a sophisticated and accurate three dimensional static Hartree-Fock

calculation, we also have a corresponding consistent dynamic calculation. A coherent description of static ground state properties, such as binding energies and deformations, is given along with a description of the collective modes of nuclei. This feature is important in studies of  $\beta$ -decay, where calculated reaction rates are very sensitive to the deformation properties of the nucleus.

A collocation basis spline lattice representation is used, which allows for a much more accurate representation of the gradient operator and hence a correspondingly accurate overall calculation. Pairing correlations can be easily included into both the static and dynamic calculation, thus enabling us to look at quasi-RPA collective effects.

Example calculations of  $^{16}\text{O}$  are presented for the response functions corresponding to various isoscalar and isovector multipole moments. It is found that the time-evolution of the system in this full three dimensional calculation contains some dependences upon the box size, which need to be addressed.

## Acknowledgements

This work was performed in part under the auspices of the U. S. Department of Energy under contracts No. DE-AC05-84OR21400 with Martin Marietta Energy Systems, Inc. and DE-FG05-87ER40376 with Vanderbilt University. This research has been supported in part by the U.S. Department of Energy, Office of Scientific Computing under the High Performance Computing and Communications Program (HPCC) as a Grand Challenge titled “the Quantum Structure of Matter”.

## References

- [1] C. R. Chinn, J. Dechargé and J.-F. Berger, ‘Correlations in a Many-Body Calculation of  $^{11}\text{Li}$ ’, to be submitted to Phys. Rev. **C**.
- [2] J. Blocki and H. Flocard, Phys. Lett. **85B**, 163 (1979).
- [3] A. S. Umar, M. R. Strayer, P. -G. Reinhard, K. T. R. Davies, and S. -J. Lee, Phys. Rev. C **40**, 706 (1989).
- [4] K. T. R. Davies and S. E. Koonin, Phys. Rev. C **23**, 2042 (1981).
- [5] P. Hoodbhoy and J. W. Negele, Nucl. Phys. **A288**, 23 (1977).
- [6] S. E. Koonin, K. T. R. Davies, V. Maruhn-Rezwani, H. Feldmeier, S. J. Krieger, and J. W. Negele, Phys. Rev. C **15**, 1359 (1977).
- [7] C. De Boor, *Practical Guide to Splines*, (Springer-Verlag, New York, 1978).
- [8] C. Bottcher and M. R. Strayer, Ann. of Phys. **175**, 64 (1987).
- [9] A. S. Umar, J. Wu, M. R. Strayer and C. Bottcher, J. of Comp. Phys. **93**, 426 (1991).
- [10] C. Bottcher, M. R. Strayer, A. S. Umar, and P. -G. Reinhard, Phys. Rev. A **40**, 4182 (1989).
- [11] A. S. Umar, M. R. Strayer, R. Y. Cusson, P.-G. Reinhard, and D. A. Bromley, Phys. Rev. C **32**, 172 (1985).
- [12] A. L. Fetter and J. D. Walecka, Quantum Theory of Many-Particle Systems, (St. Louis: McGraw-Hill Book Co., 1971).
- [13] C. R. Chinn, A. S. Umar, and M. R. Strayer, ‘Time-Dependent Evaluation of Linear Response Theory’, to be submitted to Phys. Rev. **C**.
- [14] A. S. Umar, M. R. Strayer, J.-S. Wu, D. J. Dean and M. C. Güçlü, Phys. Rev. C **44**, 2512 (1991).
- [15] T.R. Werner, J.A. Sheikh, W. Nazarewicz, M.R. Strayer, A.S. Umar and M. Misu, “Shape Coexistence Around  $^{44}\text{S}_{28}$ : The Deformed  $N = 28$  Region”, submitted to Phys. Lett.
- [16] S. Krewald, V. Klemt, J. Speth and A. Faessler, Nucl. Phys. **A281**, 166 (1977).
- [17] J. Bartelm, O. Quentin, M. Brack, C. Guet and H. B. Hakansson, Nucl. Phys. A **386**, 79 (1982).
- [18] N. Van Giai and H. Sagawa, Nucl. Phys. **A371**, 1 (1981).
- [19] P. Ring and P. Schuck, The Nuclear Many-Body Problem, (New York: Springer-Verlag 1980).

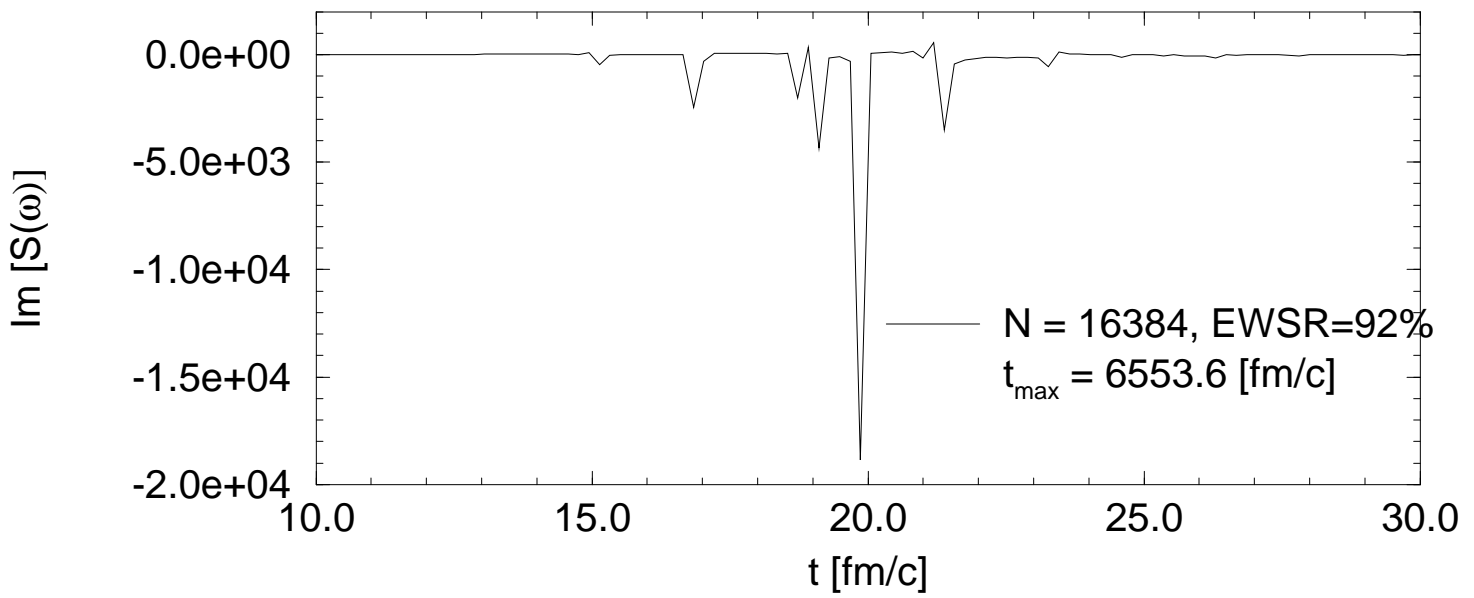
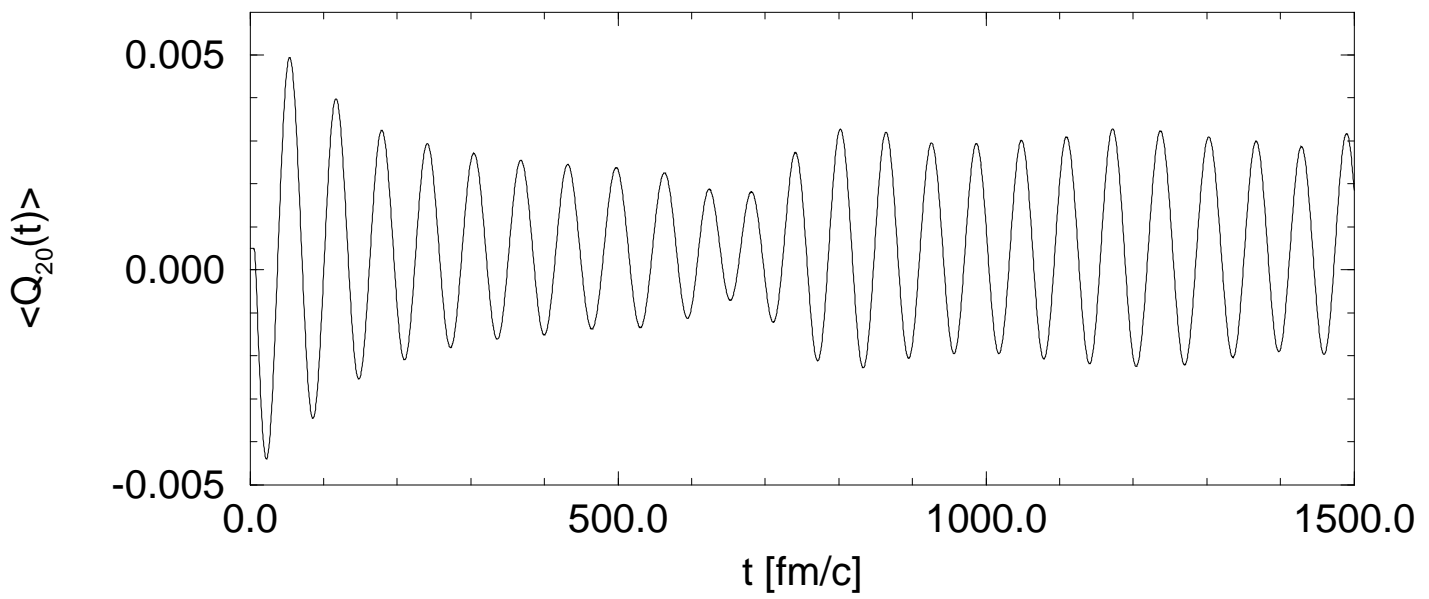
- [20] H. C. Pradhan, Y. Nogami and J. Law, Nucl. Phys. **A201**, 357 (1973); Y. Nogami, Phys. Rev. **134**, B313 (1964).
- [21] Y. Gambhir, P.-G. Reinhard, Ann. Phys. (Leipzig) **1** (1992), page 598; P.-G. Reinhard, Ann. Phys. (Leipzig) **1** (1992), p 632; P.-G. Reinhard, private communication.
- [22] K. T. Knöpfle, G. J. Wagner, H. Breuer, M. Rogge, C. Mayer-Böricke, Phys. Rev. Lett. **35**, 779 (1975).

### Figure Captions

- Fig. 1 The fluctuations in the isoscalar axial quadrupole moment as a function of time are shown in the upper panel for  $^{16}\text{O}$  using the skm\* effective interaction for 16384 time steps. The size of the time step is 0.4 fm/c with a spatial grid of  $20^3$  in a cartesian box dimensioned  $(-10, +10 \text{ fm})^3$ . The response for this calculation is shown in the lower panel.  $S(\omega)$  is obtained by fourier transforming the upper panel result and then dividing by  $f(\omega)$ .
- Fig. 2 The lower panel of Fig. 1 is repeated here in the upper panel. The middle and lower panels correspond to the same calculation as shown Fig. 1 except the box sizes are  $(-11, +11 \text{ fm})^3$  and  $(-12, +12 \text{ fm})^3$ , respectively and the grid lattices are  $22^3$  and  $24^3$ , respectively. The number of time steps used,  $N$  are labeled on the graphs.
- Fig. 3 The same as Fig. 2, except the sgII parametrization of the Skyrme force is used and the number of time steps in the time evolution is different. Also shown in the middle panel as the dashed curve is a calculation using a  $22^3$  lattice with a box size of  $(-10.6, +10.6 \text{ fm})^3$ .
- Fig. 4 The imaginary part of the response function corresponding to the isoscalar octupole moment is shown for  $^{16}\text{O}$  and executed for 16384 time steps. The skm\* and sgII parametrizations of the Skyrme force are used in the upper and lower panels, respectively with varying lattice grid and box sizes as labelled in the figure.

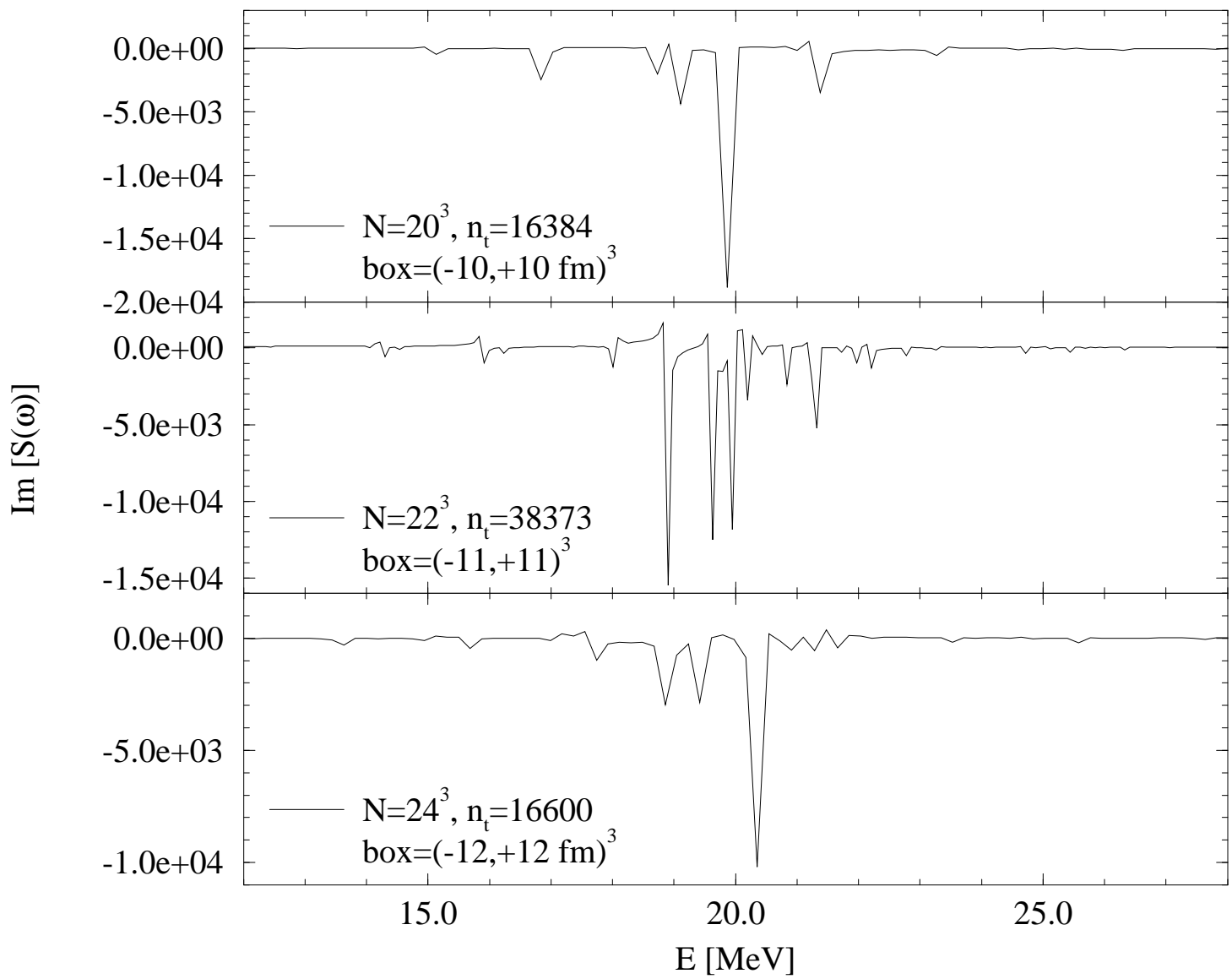
This figure "fig1-1.png" is available in "png" format from:

<http://arxiv.org/ps/nucl-th/9410034v1>



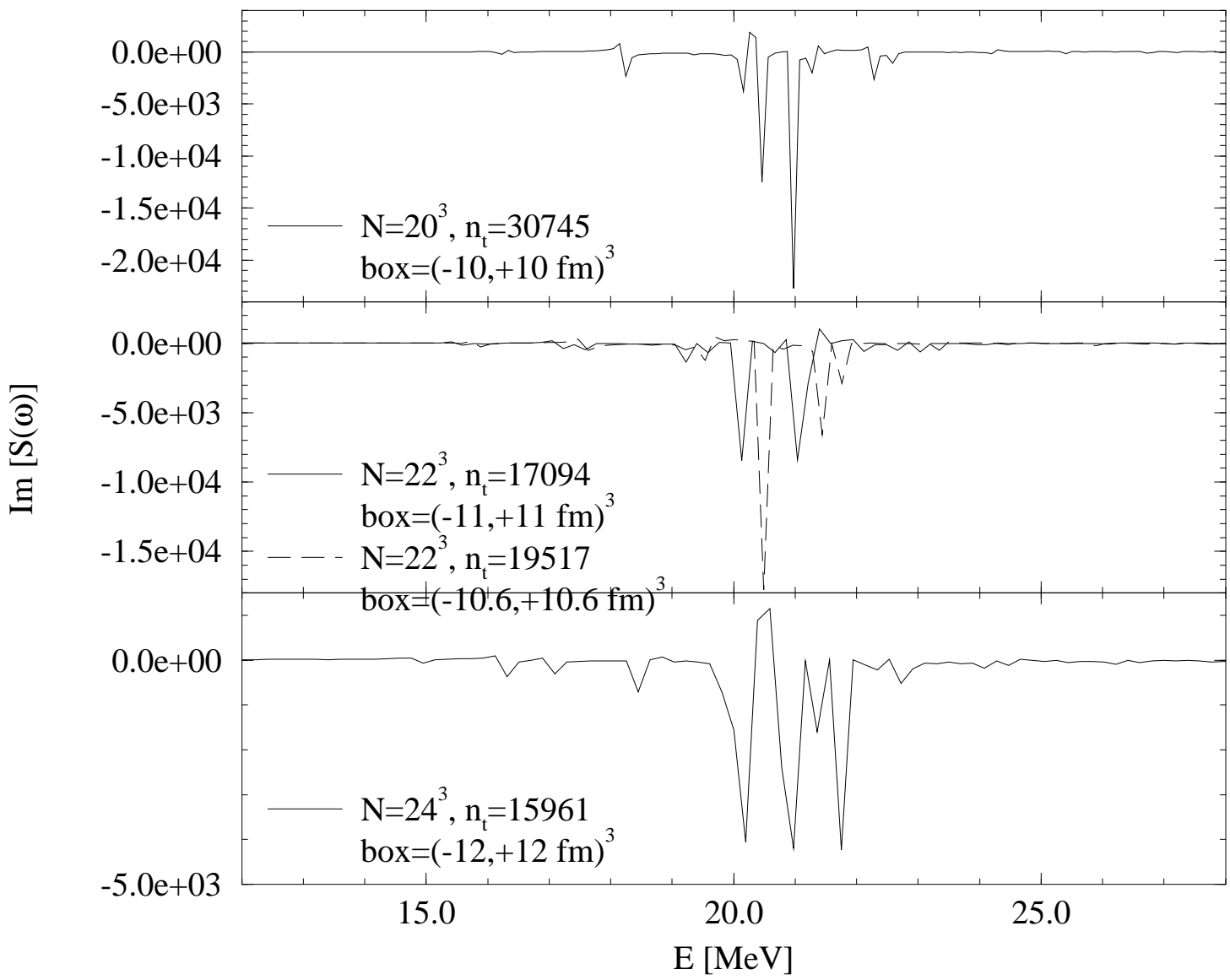
This figure "fig1-2.png" is available in "png" format from:

<http://arxiv.org/ps/nucl-th/9410034v1>



This figure "fig1-3.png" is available in "png" format from:

<http://arxiv.org/ps/nucl-th/9410034v1>



This figure "fig1-4.png" is available in "png" format from:

<http://arxiv.org/ps/nucl-th/9410034v1>

